Novel species of the oomycete Olpidiopsis potentially threaten European red algal cultivation

Yacine Badis, Tatyana Klochkova, Martina Strittmatter, Andrea Garvetto, Pedro Murúa, J. Craig Sanderson, Gwang Hoon Kim, Claire Gachon

Novel species of the oomycete *Olpidiopsis* potentially threaten European red algal cultivation

Yacine Badis[1], Tatyana A. Klochkova[2], Martina Strittmatter[1,3], Andrea Garvetto[1] , Pedro Murúa[1,4] , J. Craig Sanderson[5], Gwang Hoon Kim[6], Claire M.M. Gachon[1]

[1] The Scottish Association for Marine Science, Scottish Marine Institute, Oban, Argyll PA37 1QA, United Kingdom; [2] Kamchatka State Technical University, Petropavlovsk-Kamchatsky, 683003, Russia; [3] Roscoff Biological Station, Place Georges Teissier, 29680 Roscoff, France; [4] Aberdeen Oomycete Laboratory, College of Life Sciences and Medicine, University of Aberdeen, Foresterhill, Aberdeen, AB25 2ZD, United Kingdom; [5]Institute of Marine and Antarctic Studies, University of Tasmania, Hobart, Australia; [6]Department of Biology, Kongju National University, Kongju 32588, Korea

Author for correspondence: claire.gachon@sams.ac.uk

Tel: 0044 16 31 559 318

Abstract

The rapid growth of marine macroalgal cultivation amplifies the potential impacts of seaweed diseases. Here, we combine microscopy and molecular analysis to describe two novel European species, *Olpidiopsis palmariae* and *O. muelleri* spp. nov., that infect the commercially important red algae *Palmaria* and *Porphyra*, respectively. A Scottish variety of *Olpidiopsis porphyrae*, a devastating pathogen of *Pyropia* previously thought to be restricted to Japanese seaweed farms, is also described as *O. porphyrae* var. *scotiae*. In the light of their destructiveness in Asian farms, together with the global expansion of algal cultivation and pertaining seed trade, *Olpidiopsis* pathogens should be treated as a serious threat to the sustainability of red algal aquaculture. Our findings call for the documentation of seaweed pathogens and the creation of an international biosecurity framework to limit their spread.

Keywords:

Aquaculture, Algal Disease, Algal Parasite, Barcoding, Biosecurity, Olpidiopsis, Oomycete, Rhodophyte.

Introduction

In the last 25 years, the production of *Pyropia* (formerly *Porphyra*), the alga extensively used as sushi wrap in Asiatic cuisine, has more than tripled, mostly due to a rapid expansion in China and Korea (FAO 2014, http://www.fao.org). Over the same period, the production of seaweeds grown for their jellifying properties (carageenophytes and agarophytes, including eucheumatoids and *Gracilaria*) has increased fifteen-fold. Many more species, including *Palmaria palmata* (traditionally eaten as dulse in the UK) are subjected to cultivation trials.

A recent analysis conducted in Korea showed that alongside the intensification of production, disease management is a growing concern for farmers, and now contributes up to half the running cost of a farm (Kim *et al.*, 2014); in the last three years, three new species of pathogens infecting *Pyropia* have been described (Kim *et al.*, 2016; Klochkova *et al.*, 2016b). This echoes a well-known pattern in agriculture and animal aquaculture, whereby diseases are discovered when species first become cultivated in large scale (e.g. for invertebrate aquaculture, Brasier, 2008; Stentiford *et al.*, 2011; Stentiford *et al.*, 2017). Therefore, the identification and characterisation of pathogens infecting algal crops is becoming a research priority to underpin the sustainable development of the industry (Cottier-Cook *et al.*, 2016). To ensure the conservation of native algal biodiversity, it is also indispensable to understand the potential disease-mediated interplay between crops and wild stocks (e.g. presence of pathogen reservoirs and wild-crop cross-contamination, Loureiro *et al.*, 2015).

Amongst the most devastating pathogens of Asian *Pyropia* farms are the oomycetes *Olpidiopsis porphyrae* and *O. pyropiae*, that are investigated in Japan and Korea *(*Arasaki*,* 1947 *;* Arasaki*, 1960;* Park *et al.,* 2001*;* Ding *et al.,* 2005*;* Sekimoto *et al.,* 2008*;* Kim *et al.,* 2014*;* Klochkova *et al.,* 2016a*;* Kwak *et al.,* 2017*)*. Additionally, *Olpidiopsis bostrychiae* was found infecting *Bostrychia moritziana*, a small red alga of the West Indian Ocean mangroves (West *et al.*, 2006; Sekimoto *et al.*, 2009). Recently, records of *Olpidiopsis feldmanni* and *Olpidiopsis heterosiphoniae* were also published (Fletcher *et al.*, 2015; Klochkova *et al.*, 2017). To date, these marine endoparasites of red algae are the only members of the *Olpidiopsis* genus characterised both molecularly and morphologically; they form a monophyletic clade (commonly recognised as the order Olpidiopsidales),

most closely related to the Anisolpidiales and Haliphthorales (Gachon *et al.*, 2017). Additional older records of holocarpic pathogens of red algae have been reviewed elsewhere (Dick, 2001; Beakes *et al.*, 2014), but molecular information is lacking for all of them. Likewise, and despite their destructiveness in Asia, there is no morphology-based nor any molecular report of *Olpidiopsis* pathogens of red algae in Europe.

Taking into account the growing number of seaweed cultivation initiatives in European waters, we set out to assess if the genus *Olpidiopsis* could represent a potential threat to this developing aquaculture sector. Here, a modest sampling campaign of wild algal populations and *Palmaria* cultivation facilities led us to the identification in Scotland of two novel *Olpidiopsis* species, and of one species previously only reported in Japan (Sekimoto *et al.*, 2008).

Methods

Biological material

Details of all records of marine *Olpidiopsis* and their respective hosts ae are given in Table S1, alongside with sampling location, GPS coordinates, host culture collection ID, and Genbank sequence accession number (when applicable).

Palmaria palmata blades were collected from cultivation lines seeded in the wild (Isle of Kerrera, Scotland, UK) in April 2015 and cultivated in 10.000 L fibreglass tanks for two months (ambient light and temperature, continuous flow of seawater 7L/min). Fertile *Palmaria* tetrasporophytes developed in those conditions, together with epiphytic *Ectocarpus* filaments. *Olpidiopsis* Isolate 1 was encountered parasitizing *Palmaria* tetraspores retained on epiphytic *Ectocarpus* filaments. Though stable cultures were not established, the pathogen was successfully propagated into healthy tetraspores as follows: healthy fertile tetrasporophytes were rinsed and maintained overnight at 10^{o}C in filtered sterile sea water, and a tetraspore suspension was obtained by gentle centrifugation (2000g for 10min at 10^{o}C). In an inoculation procedure adapted from Strittmatter *et al.* (2013), a droplet of healthy tetraspore suspension was placed in a 50 mm diameter, 20 mm-deep petri dish, covered with a 40-μm mesh cell strainer containing the infected material. The propagation of the parasite into the tetraspores beneath the cell strainer was monitored by bright field microscopy and this material was used for histological staining and DNA extraction.

***Porphyra* sp.** blades infected with several *Olpidiopsis* parasites were collected from various locations in Scotland (Table S1), namely the Shetland Islands (Isolate 2), Seil Island (Isolate 4) and Oban.

***Polysiphonia* sp.** specimens (infected with *Olpidiopsis* Isolate 3) were collected at low tide (Clachan Bridge, Scotland, UK) and observed using conventional bright field microscopy (Zeiss Observer Z1). Infected algal tips were dissected for subsequent DNA extraction.

Histological staining

Observations were made on fresh material, or samples fixed in 2% formaldehyde and 0,2% glutaraldehyde in phosphate buffered saline). Cell wall structures and nuclei were stained with Calcofluor white and SYBR-Green, respectively (Gachon *et al.*, 2017).

DNA extraction sequencing and molecular phylogeny reconstruction

DNA extraction of infected *Palmaria* tetraspore suspensions, infected *Porphyra* sp., and infected *Polysiphonia* algal tips was performed according to Strittmatter *et al*. 2013. Oomycete Cox1, Cox 2 and 18S markers were amplified (according to Gachon *et al.*, 2017) and individually subjected to phylogeny reconstruction with a representative subset of published oomycete sequences. NCBI accession numbers of all sequences used for phylogeny reconstruction are given in Table S2. Alignments were generated using the MAFFT algorithm and manually corrected prior to phylogenetic analysis in MEGA v. 7 (Kumar *et al.*, 2016). Model tests were performed on each alignment prior to maximum likelihood (ML) analysis to find the best substitution models. For the 18S rRNA, Tamura-3-parameter was used (Tamura, 1992) with a discrete Gamma distribution to model evolutionary rate differences among sites. The model by Le & Gascuel was used with discrete gamma distribution for cox1 and cox2 markers (Le *et al.*, 2008). The rate variation model allowed for some sites to be evolutionarily invariable for the cox2 alignment. Maximum parsimony analysis was also performed on all three datasets. Bootstrap re-sampling was set to 500 replicates. *Palmaria* and *Polysiphonia* SSU markers were amplified using primers according to Saunders *et al*. (2013), and default Neighbour Joining trees were generated in Geneious R6 (Fig. S7).

Results and discussion

A novel Olpidiopsis pathogen identified in Palmaria palmata cultivation facilities

Isolate 1, hereafter identified as *O. palmariae* sp. nov., was discovered when monitoring fertile *Palmaria palmata* tetrasporophytes grown in tanks (Fig. 1a,b and Fig. S1a). The blades were colonised by brown filamentous epiphytes (*Ectocarpus* sp.) and displayed an unusual punctuated aspect due to the germination of tetraspores before their release (Fig S1b). Numerous free *Palmaria* tetraspores, as well as some young gametophytes (Fig. 1b), were found entangled in the brown filamentous epiphytes. Most tetraspores appeared dead and devoid of any cellular content, suggestive of an infection with an intracellular holocarpic pathogen (arrows on Fig. 1b). Various developmental stages of

the parasite thallus were observed (Fig. 1c-h): young unwalled thalli in degrading red algal cell structures (Fig. 1c), as well as older, granulous thalli filling entirely dead *Palmaria* tetraspores (arrow on Fig. 1d). Each granular thallus developed an exit tube in the course of spore differentiation (arrowhead on Fig. 1e). Some dead *Palmaria* tetraspores contained mature pathogen sporangia with individualised encysted spores (Fig. 1f) and multiple infections of the same tetraspore were frequent (Fig. 1g-h). Each mature empty sporangium displayed one single exit tube of varying length (Fig. 1h). We successfully propagated the pathogen by co-incubating infected material with freshly released *Palmaria* tetraspores, enabling us to better observe its development (Fig. 2). Uninfected tetraspores had a granulous content, with often an asymmetric repartition of chloroplasts (Fig. 2a). We did not succeed in observing the penetration of the pathogen into the red algal cell, and the earliest recognisable stage of infection was characterised by a small refringent globule (ca. 2 µm in diameter) surrounded by a spherical structure within the tetraspore cytosol (Fig. 2b). We assume that this perfectly spherical shape is conferred by a prominent vacuole (arrow on Fig. 2c) that occupies most of the thallus biovolume. Small vesicles (arrowheads on Fig. 2c) appeared at this stage. Each thallus grew outwards very rapidly, as shown in a 21 min time course (Figs. 2d to 2f). During this period, increasing digestion of the red algal cell structures was evident and absorption vesicles formed at the algal-pathogen interface, suggestive of rapid incorporation of algal material by the parasite. The diameter of the absorption vesicles increased with time, and they fused with the central globule (arrowheads on Fig. 2e and 2f), suggesting that the latter is a storage structure. Once the tetraspore content was fully assimilated, each thallus differentiated a cell wall (arrow on Fig. 2g) and underwent radical ultrastructural changes. The refringent globule and the vacuole both receded in size and became fragmented, leaving space for an increasingly dense cytosol (Fig 2g-h). Just before sporogenesis, only dense cytoplasm was recognisable in the once highly vacuolated thallus (Fig. 2i).

SYBR Green staining revealed that walled thalli are multinucleate syncytia (Fig. 3a): Similar to recent observations conducted on the closely related pathogen *Anisolpidium ectocarpii* (Gachon *et al.*, 2017), the nuclei of the younger stages were ca. 2.5 µm in diameter with condensed peripheral material (arrowheads), whereas more mature stages had dense compact nuclei ca. 1 µm in diameter (arrow). All nuclei within a

thallus were always at the same stage, therefore we assume that nuclear divisions are synchronous, as is often the case in syncytial organisms. Multiple infections of the same tetraspores were prevalent in our co-incubation experiment. In tetraspores containing multiple parasites, SYBR Green and calcofluor white staining did not hint to sexual fusion between antheridia and oogonia (Fig. 3b and c). Each sporangium produced one exit tube. Calcofluor staining revealed that the length of the exit tubes varied widely from 3 to ca. 20 µm (Fig. 3d, the inset shows the same infected spore in a different focal plane). Remnants of encysted spores were observed on the surface of some host cells. Those were 3 µm in diameter and had a thin, calcofluor-positive cell wall (Fig. 3e). Very thin needle-like structures reminiscent of the penetration structure of *A. ectocarpii* (Gachon *et al.*, 2017) were observed, through which spore content was injected into the *Palmaria* host (arrowheads on fig 3e). It is unclear whether these infectious spores encyst at the surface of the algal host directly following their release from the sporangium, or if diplanetism might exist.

Comparable to other holocarpic oomycetes, the syncytium segmented to produce spores (Fig. 2g-i). The dehiscence of one pathogen sporangium was observed, as well as subsequent spore differentiation (Fig. 3f-h). Spores were about 3 µm in diameter and assumed a light amoeboid movement inside the sporangium. Their release outside the sporangium took a few minutes. As soon as the spores reached the outside medium, they extended two straight flagella of unequal length within a minute or less (Fig. 3f and g). During this process, the spores first assumed a triangular shape (Fig. 3f) and progressively became spherical (h and i). The mature flagella were 3 and 8-10 µm, respectively, and bore a vesicle at their apex and tips (Fig. 3f-i, white arrowheads), probably due to rapid reorganisation of their plasma membrane.

To the exception of individual cells of developing female gametophytes, no infection was observed on any of the other *Palmaria* life stage available in culture (tetrasporophytes, and embryos). In the absence of a stable supply of *Palmaria* tetraspores, this stage-specificity of the parasite prevented its long-term laboratory cultivation. Morphologically similar parasites were observed again several times in other populations of *Palmaria palmata* grown in tanks, and on September 7th, 2015 on individuals collected in Seil Island (Supplementary Table S1).

A novel Olpidiopsis parasite infecting both wild Porphyra and Polysiphonia

Isolate 2, hereafter identified as *O. muelleri* sp. nov.*,* stemmed from a female gametophyte of *Porphyra* sp. harvested in the Shetland Islands due to its discoloured margin (Fig. S1c,d). The infection was spatially restricted to the fertile margin where red female gametes could still be found (Fig. 4a, arrowheads). The pathogen thalli were granular and completely filled their host algal cell, which displayed an almost spherical shape and altered brownish to greenish pigmentation (arrows). Each of the sporangia developed a single and highly vacuolated exit tube (inset on Fig. 4b). Calcofluor white staining of the same infected margin revealed a high density of infection (Fig. 4b, main picture), and highlighted numerous *Olpidiopsis* empty sporangia with exit tubes of varying length (ca. 20-80 µm). We did not observe any evidence of multiple infections of the same algal cell. Numerous additional observations of *Olpidiopsis* parasitizing *Porphyra sp.* were recorded from various blades collected in Oban and its surrounding (Fig. S2) but they were not submitted to DNA barcoding.

Isolate 3, hereafter identified as *O. muelleri* var. *polysiphoniae,* was observed on *Polysiphonia stricta*. The host alga displayed slightly curved growing tips (Fig. 4c), of which several were infected (Fig. 4d). The parasite first developed as an apparently unwalled granulous syncytium with granulous, greyish content which sometimes completely filled the infected algal tip (Fig. 4d); spanning several algal cells, the cell wall of which was still discernible (arrowheads on Fig. 4e). When infecting three-dimensionally branched algal tips, the parasite thallus was lobed (arrow on e). Multiple and perfectly spherical vacuoles could often be seen (Fig. 4f). The vacuolated thalli displayed a clearly-defined wall (arrow). Additional smaller unwalled thalli could be found in the same infected tip (arrowheads), suggesting multiple infections. Mature parasite sporangia with individualized spores of ca. 5 µm in diameter were also observed (Fig. 4g). Remains of excysted spore cell walls reminiscent of the honeycomb structure typical of *Eurychasma* could be observed within empty sporangia (Fig. 4h), and the latter typically displayed one or two short exit tubes (arrows in Fig. 4h). This honeycomb structure is suggestive of sequential spore encystment/excystment, and therefore of diplanetism. Spore release was not observed, and in the absence of potential alternative hosts, the limited material prevented us from documenting further the life cycle of this parasite.

A new variety of Asian Olpidiopsis parasite is present in Scotland

Isolate 4, hereafter molecularly identified as *O. porphyrae* var. *scotiae*, was observed on wild *Porphyra* blades collected from Easdale, Argyll, Scotland. Infected blades were crinkled (Fig. S1e), resulting from localised necrotic lesions (arrows on Fig. S1f). Diseased tissue revealed patches of infected host cells (Fig. 5a and higher magnification on Fig. 5b). *Porphyra* cells containing pre-mature parasite thalli appeared light pink due to degradation of algal pigments (dark arrows). The parasite thallus ultimately filled the host cell, where remaining greenish algal material was compacted at the periphery (dark arrowheads). The centre of infected patches usually displayed collapsed dead cells of *Porphyra* (double arrowheads). Multiple infections of the same host cell were frequently observed (Fig. 5c). In such multiple infections, calcofluor staining of the parasite cell wall did not reveal any thallus fusion (inset in Fig. 5c), although further ultrastructural work is needed to ascertain this result. Neighbouring dead collapsed *Porphyra* cells (double arrowheads in Fig. 5c) were also calcofluor-positive, thus revealing empty parasite sporangia. All empty sporangia observed displayed single exit tubes of varying length (ca. 5-30 µm). SYBR-Green staining revealed fully grown syncytial sporangia containing numerous nuclei (Fig. 5d). The number of nuclei (and thus of infectious propagules) seemingly depended on the overall size of differentiating sporangia, although no precise quantification was attempted. Diseased material was incubated with fresh spores released by the same blade, leading to the observation of successful spore infections (Fig. 5e).

Molecular phylogeny unveils two novel *Olpidiopsis* species and unknown varieties of Asian *Olpidiopsis* strains

18S sequences were obtained for all four isolates described above. We were also successful in obtaining a Cox2 sequence for Isolates 2 and 4 and a Cox1 sequence for Isolate 4. All sequences generated in this study were submitted to Genbank (Table S1) and used for Maximum Likelihood and Maximum Parsimony tree reconstruction (Fig. 6 and Fig. S3). All markers consistently grouped our four isolates with the known marine *Olpidiopsis* parasitizing red algae, within a single clade (red arrow on Fig. 6 and Fig. S3), most closely related to *Haliphthoros, Halocrusticida* and *Halodaphnea* (Haliphthorales). Though the bootstrap values are mediocre, our 18S data further suggest that marine *Olpidiopsis* species are split in three distinct clades, that we hereafter refer to as the

"bostrychiae", "*pyropiae*" and "*porphyrae*" lineages. The parasite of *P. palmata* (Isolate 1) was most closely related to *O. porphyrae,* with 98.8% identity on exons of the 18S sequence. Its unique host, zoospore differentiation and 18S sequence set it aside from *O. porphyrae* and we therefore propose to name it *Olpidiopsis palmariae* sp. nov. The 18S sequence obtained for Isolate 2 was closest to *O. bostrychiae* (97% identity, AB363063.1) while the amino acid Cox2 sequence formed a long branch clustered with *O. porphyrae* (85% identity versus 72% identity with *O. bostrychiae*, Fig. S5). Therefore, we conclude that isolate 2 is a novel species that we name *Olpidiopsis muelleri* sp. nov. While no Cox2 sequence was obtained for the *Polysiphonia* parasite Isolate 3, its 18S sequence was 100% identical to *O. muelleri* (Isolate 2). In contrast to all members of the "*bostrychiae"* and "*porphyrae"* lineages, Isolate 3 forms honeycomb structures strongly suggestive of diplanetism. This specific phenology argues against Isolate 3 being conspecific with any of the *Olpidiopsis* already described, especially *O. muelleri*. However, we were unable to observe zoospore behaviour on *O. muelleri* (Isolate 2). Therefore, our conservative interpretation is to consider Isolates 2 and 3 as conspecific until more molecular or morphological evidence is obtained. In order to take into account its different host and phenology compared to Isolate 2, we refer to Isolate 3 as *O. muelleri* var. *polysiphoniae.* Finally, the 18S and Cox1 sequences of Isolate 4 were 100% identical to *O. porphyrae.* Its virtually translated Cox2 sequence was 99.4% identical to *O. porphyrae* (one substitution over 180 amino acid residues). Introns were also detected in the 18S sequence, some of which were conserved with *O. porphyrae* and/or with *O. porphyrae* var. *koreanae* (Fig. S6). Taking into account its original intron-exon structure, a feature already used to erect the Korean variety *O. porphyrae* var. *koreanae* (Kwak *et al.*, 2017), we refer to this isolate as *O. porphyrae* var. *scotiae*.

Conclusion

Here we describe two pathogens, *Olpidiopsis palmariae* and *O. muelleri* spp. nov. and report two novel varieties *O. muelleri* var. *polysiphoniae* and *O. porphyrae* var. *scotiae* from Scotland. In the light of our modest sampling efforts, this work illustrates the widespread occurrence of undocumented *Olpidiopsis* species infecting both wild and cultivated algae in Europe. The destructiveness of *O. pyropiae* and *O. porphyrae* in Asia demonstrates the risk posed by these oomycete pathogens for the red seaweed industry (Ding and Ma, 2005; Kim *et al.*, 2014; Kwak *et al.*, 2017). Accordingly, disease

management has become an integral part of farm design and operation in Asia; most recently, insurance schemes have been set-up to protect farmers against worsening crop losses (Cottier-Cook *et al.*, 2016). Our repeated observations of *O. palmariae* in cultivation facilities in Scotland, combined with multiple accounts by growers of hitherto unexplained seeding failures, highlights the real possibility of yield-limiting epidemic outbreaks in the nascent Western aquaculture industry, and echoes repeated reports of *Petersenia* diseases in Canadian *Chondrus* production facilities (Craigie *et al.*, 1996 and refs therein). This first European report of an *Olpidiopsis* species which is already known to be highly destructive in Asia, opens the question of the potential economic impact that non-native pathogens could have on Asian crops, especially if they were introduced as a result of unregulated seed movements. Taken together, our findings call for a much more systematic documentation of seaweed pathogens and the creation of an international biosecurity framework to monitor and limit their spread.

Taxonomy

Olpidiopsis palmariae **Y. Badis & C.M.M. Gachon sp. nov.**

Vegetative thalli endobiotic, spherical, 2.3–4 µm in diameter when young, 10–50 µm before cell-wall thickening and zoospore cleavage; completely filling host cell at maturity, single discharge tube of variable length (3.5 to 30 µm) protruding from the algal tetraspore; Multiple infections frequent (typically 2-5 thalli in one host cell in holotype material), resulting in angular sporangia after cell wall thickening; zoospores maturing outside of zoosporangium, triangular to spherical at maturity, 2.5–3.5 µm in diameter, laterally biflagellate; flagella perpendicular and of unequal length (3 and 8-10 µm, respectively), differentiating upon discharge of the spores from the sporangium and bearing at least temporarily submicrometric vesicles at their apical extremity; resting spores unknown; obligate endoparasite in *Palmaria palmata* (Rhodophyceae). Only observed infecting tetraspores or very young (2-8 cells) gametophytes.

HOLOTYPE: Registration number BM001222129 (Population of infected *Palmaria* tetraspores in formaldehyde/glutaraldehyde TEM buffer), National History Museum, London (NHM). Type specimens are specific of *Palmaria palmata* tetraspores.

ILLUSTRATIONS WITH ANALYSIS: Fig. 2

PARATYPES: MuseumID (resin-embedded EM specimen), National History Museum, London (NHM).
TYPE LOCALITY: Kerrera Island, Oban, Scotland, United Kingdom.
TYPE CULTURE: None
ETYMOLOGY: Named after its algal host.
GenBank accession number: KY403502 (18S)

***Olpidiopsis muelleri* Y. Badis & C.M.M. Gachon sp. nov.**

Vegetative thalli endobiotic, spherical, 10–50 µm in diameter and zoospore cleavage; completely filling host cell at maturity; single vacuolated discharge tube (variable length, 20 to 80 µm) protruding from the host algal cortex at maturity; zoospores not observed; obligate endoparasite in *Porphyra* sp. gametophyte.
HOLOTYPE: Registration number BM001222128 (Fragment of infected *Porphyra* blade (Fig. S1.c-d) in formaldehyde/glutaraldehyde TEM buffer), National History Museum, London (NHM).
ILLUSTRATIONS WITH ANALYSIS: Fig 4a-b.
ISOTYPES: Additional fragment of the same infected *Porphyra* blade (Fig. S1.c-d) in formaldehyde/glutaraldehyde TEM buffer), National History Museum, London (NHM).
TYPE LOCALITY: Lunna, Shetland Islands, Scotland, United Kingdom. (60°24'; -1°07')
TYPE CULTURE: None.
ETYMOLOGY: Named after Professor Dieter. G. Mueller, in recognition of his pioneering contribution to the study and laboratory cultivation of marine oomycetes.
Genbank accession numbers: KY403503 (18S) and KY403508 (Cox2)

***Olpidiopsis muelleri* var. *polysiphoniae* Y. Badis & C.M.M. Gachon var. nov.**

Vegetative thalli endobiotic, elongated, 10–50 µm, restricted to algal tips, completely filling several adjacent cells, causing slight hypertrophy of algal tips, possibly lobed in bifurcated algal tips; thalli naked in early stages, walled and vacuolated in later stages; 1-2 short discharge tubes (5 µm) protruding from the host algal cortex at maturity; Zoospores sub-spherical, 3 to 5 µm in diameter, diplanetic, maturing and encysting in sporangium. Remains of excysted spore cell walls visible in empty sporangium, forming an irregular honeycomb structure. Obligate endoparasite in apices of *Polysiphonia* sp.

ICONOTYPE: Fig. 4c-h

TYPE LOCALITY: Atlantic Bridge, Seil Island, Scotland, United Kingdom. (56°17'; -5°58')

TYPE CULTURE: None.

ETYMOLOGY: Named after *Olpidiopsis muelleri*, on the basis of its identical 18S sequence, and the specific host of this isolate.

Genbank accession number: KY403501 (18S).

***Olpidiopsis porphyrae* var. *scotiae* Y. Badis, G.H. Kim, T.A. Klochkova & C.M.M. Gachon var. nov.**

Vegetative thalli endobiotic, spherical to ellipsoidal, 2.5–6 µm in diameter when young, 12–30 µm in size when mature before spore cleavage; with 1 discharge tube protruding from the host algal cortex at maturity. Zoospores spherical to reniform, 2.2–3.5 µm in size, biflagellate, motile, maturing in sporangium; two flagella of unequal length, inserted sub-apically, positioned at 45o angle. Dormant cysts spherical to ovoid, non-motile, without flagella, maturing in sporangium. Armored resting spores absent; sexual reproduction absent. Obligate endoparasite in *Porphyra* and *Pyropia* spp. 18S rRNA gene sequence contains 5 group I introns.

COLLECTION: Oban, Scotland; May 2016; by Kim G.H.

ICONOTYPE: Fig. 5

TYPE LOCALITY: Seil Island, Scotland, United Kingdom. (56°17'; -5°39')

ETYMOLOGY: Named after *Olpidiopsis porphyrae*, and the type locality of this isolate.

GenBank accession number: KY403504 (18S), KY403506 (cox1), KY403505 (cox2).

Acknowledgements

This work was supported through the UK NERC IOF Pump-priming + scheme (NE/L013223/1 – Y.B./C.M.M.G.), the European Union's Horizon 2020 research and innovation (ALFF No 642575 – A.G./C.M.M.G; EMBRIC No 654008 – C.M.M.G.), the Genomia fund (HERDIR – M.S), and a MASTS Visiting Fellowship Scheme (J.C.S.). P.M. was funded by Conicyt (BecasChile N◦72130422) for PhD studies at the University of Aberdeen, and by the NERCIOF Pump-priming (scheme NE/L013223/1) for activities at the Scottish Association for Marine Sciences. This work was partially supported by a National Research Foundation of Korea Grant (NRF-2015M1A5A1041804) funded to

G.H.K. We are also grateful Duncan Smallman and Philip Kerrison for providing *Palmaria* specimens.

Author Contributions

CMMG, GHK, YB and TAK designed the experiments; CMMG and GHK supervised the research; YB, CMMG, GHK and JCS conducted the fieldwork; YB, TAK, MS, AG and PM conducted the laboratory work YB and CMMG wrote the manuscript with contributions from all co- authors. All authors gave final approval for publication.

References

Arasaki S. 1947. Studies on the rot of Porphyra tenera by a Pythium. *J. Jap Soc. Fish.*, 13:74-90.

Arasaki S. 1960. A chytridean parasite on the Porphyra. *Bull. Jap. Soc. Sci. Fish.*, 26:543-8.

Beakes G. W., Honda D. & Thines M. 2014. Systematics of the Straminipila: Labyrinthulomycota, Hyphochytriomycota, and Oomycota. *In:* MCLAUGHLIN, D. J. & SPATAFORA, J. W. (eds.) *Systematics and Evolution 2d edition The Mycota VII part A.*

Brasier C. M. 2008. The biosecurity threat to the UK and global environment from international trade in plants. *Plant Pathology,* 57, 792-808.

Cottier-Cook E. J., Nagabhatla N., Badis Y., Campbell M. L., Chopin T., Dai W.*, et al.* 2016. Safeguarding the future of the global seaweed aquaculture industry. *United Nations University (INWEH) and Scottish Association for Marine Science Policy Brief. ISBN 978-92-808-6080-1.*

Craigie J. S. & Correa J. A. 1996. Etiology of infectious diseases in cultivated Chondrus crispus (Gigartinales, Rhodophyta). *Hydrobiologia,* 326, 97-104.

Dick M. W. 2001. Straminipilous fungi: systematics of the peronosporomycetes, including accounts of the marine straminipilous protists, the plasmodiophorids, and similar organisms., pp 362-366.

Ding H. & Ma J. 2005. Simultaneous infection by red rot and chytrid diseases in Porphyra yezoensisUeda. *Journal of Applied Phycology,* 17, 51-56.

Fletcher K., Uljevic A., Tsirigoti A., Antolic B., Katsaros C., Nikolic V.*, et al.* 2015. New record and phylogenetic affinities of the oomycete Olpidiopsis feldmanni infecting Asparagopsis sp. (Rhodophyta). *Diseases of aquatic organisms,* 117, 45-57.

Gachon C. M., Strittmatter M., Badis Y., Fletcher K. I., Van West P. & Müller D. G. 2017. Pathogens of brown algae: culture studies of Anisolpidium ectocarpii and A. rosenvingei reveal that the Anisolpidiales are uniflagellated oomycetes. *European Journal of Phycology,* 52, 133-148.

Kim G. H., Klochkova T. A., Lee D. J. & Im S. H. 2016. Chloroplast virus causes green-spot disease in cultivated Pyropia of Korea. *Algal Research,* 17**,** 293-299.

Kim G. H., Moon K.-H., Kim J.-Y., Shim J. & Klochkova T. A. 2014. A revaluation of algal diseases in Korean Pyropia (Porphyra) sea farms and their economic impact. *ALGAE,* 29**,** 249-265.

Klochkova T. A., Jung S. & Kim G. H. 2016a. Host range and salinity tolerance of Pythium porphyrae may indicate its terrestrial origin. *Journal of Applied Phycology***,** 1-9.

Klochkova T. A., Kwak M. S. & Kim G. H. 2017. A new endoparasite Olpidiopsis heterosiphoniae sp. nov. that infects red algae in Korea. *Algal Research*.

Klochkova T. A., Shin Y. J., Moon K.-H., Motomura T. & Kim G. H. 2016b. New species of unicellular obligate parasite, Olpidiopsis pyropiae sp. nov., that plagues Pyropia sea farms in Korea. *Journal of Applied Phycology,* 28**,** 73-83.

Kumar S., Stecher G. & Tamura K. 2016. MEGA7: Molecular Evolutionary Genetics Analysis Version 7.0 for Bigger Datasets. *Molecular biology and evolution,* 33**,** 1870-4.

Kwak M. S., Klochkova T. A., Jeong S. & Kim G. H. 2017. Olpidiopsis porphyrae var. koreanae, an endemic endoparasite infecting cultivated Pyropia yezoensis in Korea. *Journal of Applied Phycology*.

Le S. Q. & Gascuel O. 2008. An improved general amino acid replacement matrix. *Molecular biology and evolution,* 25**,** 1307-20.

Loureiro R., Gachon C. M. & Rebours C. 2015. Seaweed cultivation: potential and challenges of crop domestication at an unprecedented pace. *The New phytologist,* 206**,** 489-92.

Park C. S., Kakinuma M. & Amano H. 2001. Detection and quantitative analysis of zoospores of Pythium porphyrae, causative organism of red rot disease in Porphyra, by competitive PCR. *Journal of Applied Phycology,* 13**,** 433-441.

Saunders G. W. & Moore T. 2013. [Review] Refinements for the amplification and sequencing of red algal DNA barcode and RedToL phylogenetic markers: a summary of current primers, profiles and strategies. *ALGAE,* 28**,** 31-43.

Sekimoto S., Klochkova T. A., West J. A., Beakes G. W. & Honda D. 2009. Olpidiopsis bostrychiae sp. nov.: an endoparasitic oomycete that infects Bostrychia and other red algae (Rhodophyta). *Phycologia,* 48**,** 460-472.

Sekimoto S., Yokoo K., Kawamura Y. & Honda D. 2008. Taxonomy, molecular phylogeny, and ultrastructural morphology of Olpidiopsis porphyrae sp. nov. (Oomycetes, straminipiles), a

unicellular obligate endoparasite of Bangia and Porphyra spp. (Bangiales, Rhodophyta). *Mycological research,* 112**,** 361-74.

Stentiford G. D. & Lightner D. V. 2011. Cases of White Spot Disease (WSD) in European shrimp farms. *Aquaculture,* 319**,** 302-306.

Stentiford G. D., Sritunyalucksana K., Flegel T. W., Williams B. A. P., Withyachumnarnkul B., Itsathitphaisarn O.*, et al.* 2017. New Paradigms to Help Solve the Global Aquaculture Disease Crisis. *PLoS Pathogens,* 13**,** e1006160.

Strittmatter M., Gachon C. M., Muller D. G., Kleinteich J., Heesch S., Tsirigoti A.*, et al.* 2013. Intracellular eukaryotic pathogens in brown macroalgae in the Eastern Mediterranean, including LSU rRNA data for the oomycete Eurychasma dicksonii. *Diseases of aquatic organisms,* 104**,** 1-11.

Tamura K. 1992. Estimation of the number of nucleotide substitutions when there are strong transition-transversion and G+C-content biases. *Molecular biology and evolution,* 9**,** 678-87.

West J. A., Klochkova T. A., Kim G. H. & Loiseaux-de Goër S. 2006. Olpidiopsis sp., an oomycete from Madagascar that infects Bostrychia and other red algae: Host species susceptibility. *Phycological Research,* 54**,** 72-85.

Figure Legends

Fig. 1 *Olpidiopsis palmariae* – Main description

a. Cultivated blade of *Palmaria palmata* with epiphytic tufts of *Ectocarpus* sp. (thick brown arrows); the rare whitish necrotic lesions (white arrow) do not seem related with the *Olpidiopsis* disease. **b**. Numerous tetraspores associated to *Ectocarpus* tufts, as well as some young gametophytes. Most tetraspores appear dead, following an infection with an intracellular holocarpic pathogen (arrows). Inset: mature sporangium within a young gametophyte that is still pigmented. **c-h**. Development stages of the pathogen. c. Two young unwalled thalli (arrows) inside a degrading tetraspore. **d.** Thick-walled granulous thallus (arrow), surrounded by two mature empty sporangia (arrowheads). **e.** Sporangium (arrow) containing differentiating spores; Note the long thin exit tube (arrowhead). **f.** Sporangium with individualised encysted spores; note the absence of honeycomb-like structure. **g.** Multiple infections of the same tetraspore are frequent. **h.**

Two empty thick-wall sporangia with exit tubes of different length (arrowheads). Bars : b. 20 µm; c-h. 10 µm.

Fig. 2 *Olpidiopsis palmariae* – Pathogen nutrition inside the tetraspore

a. Healthy tetraspore of *Palmaria palmata*. **b.** Earliest stages of infection, showing small individual globules (ca. 2 µm in diameter) surrounded by a vacuole **c.** Spherical thalli (arrow) are delimited by a vacuole and contain a refringent central globule and small absorption vesicles (arrowheads). **d-f** Time course over 20 minutes, showing rapid outward growth of each thallus (arrow); note the formation, growth of absorption vesicles at the thallus periphery, followed by their fusion with the central globule (arrowheads). **g-i**. Structural changes in differentiating sporangia: **g-h**. Pathogen cell wall differentiation in fully assimilated tetraspores; note the angular cell walls separating several pathogen thalli; the vacuole and the refringent globule then start receding, progressively leading to the granulous aspect shown in h. **i**. Initiation of cytoplasm segmentation during sporogenesis; the upper sporangium already discharged zoospores. **Legend**: Thick arrow: individual thallus; Thin arrow: Pathogen cell wall; V-shaped arrowhead: vacuole. Arrowhead: absorption vesicle and/or refringent globule. All bars: 10 µm.

Fig. 3 *Olpidiopsis palmariae* – Sporogenesis and infection structures

a. Sybr-Green staining reveals multinucleate thalli at different stages. A nucleolus is visible on younger stages nuclei (arrowheads), whereas more mature stages have dense compact nuclei (arrows). **b.** Sybr-Green (left) and calcofluor white staining (right) do not hint to thallus fusion **c.** Similar conclusions as in a-b, on a different object. **d.** Calcofluor staining of multiple sporangia showing variability in the length of the exit tubes. Inset: same infected spore in a different focal plane. **e.** Calcofluor staining showing the remains of encysted pathogen spores bearing thin injection needles (arrowheads). All bars. **f-g.** Rapid differentiation of flagella in two freshly released spores. The pictures were taken ca. 1 min apart from each other. **h-i**. Spherical spores with fully mature, straight flagella of unequal length, seen from different angles. In all pictures, the arrowhead points to the bulging membranar structure at the tip of each flagellum. Bars: a-e. 10 µm; f-i. 2 µm.

Fig. 4 *Olpidiopsis muelleri* on *Porphyra sp.* and *Polysiphonia sp.*

a. Close-up of fertile *Porphyra* sp. blade margin showing cells infected by intracellular parasites (dark arrows) and healthy female cells (arrowheads) **b**. Highly infected region stained with Calcofluor white. Note the varying length of exit tubes (up to 80 μm). Inset: Single vacuolated exit tube (arrow) produced by a by mature sporangium (arrow). **c.** Healthy filament tips of *Polysiphonia stricta* **d**. Unwalled intramatrical thallus in a filament tip of *P. stricta;* Note the tip swelling when compared to c. **e.** Lobed shape of the parasite thallus (arrow) invading several algal cells. Note the visible remnants of the host cell walls (arrowheads). **f**. Spherical vacuoles can often be seen at late stages of infection. Note the clearly-defined wall (arrow), whereas the smaller thalli to the top and bottom right are unwalled (arrowheads). **g**. Encysted spores in mature sporangium. **h.** Empty sporangium with two rather short exit tubes (arrows). Note the remains of excysted spore cell walls forming a coarse honeycomb structure. Bars: a, e-f, and inset in b. 20 μm; b. 100 μm; c-g. 50 μm; h. 10 μm.

Fig. 5 *Olpidiopsis porphyrae* var. *scotiae* on Scottish *Porphyra* sp.

a-b. Necrotic patch of infected *Porphyra* cells. Note the contrasting pigmentation of infected cells, ranging from pinkish in earlier stages (arrows) to greenish in later stages (arrowheads). Dead collapsed host cells are usually observed in the centre of each patch (double arrowheads). **c.** Multiple infections of *Porphyra* cells were frequently observed. Inset: Calcofluor staining of parasite cell wall did not reveal any thallus fusion; collapsed dead *Porphyra* cells (double arrowheads) are calcofluor positive, revealing empty pathogen sporangia. **d**. Syncytial mature sporangia revealed by SYBR-Green staining. **e.** Olpidiopsis thallus (arrow) growing in *Porphyra* spore.

Fig. 6 Molecular phylogeny of marine members of the *Olpidiopsis* genus

Maximum Likelihood inference of the phylogeny of all known *Olpidiopsis* 18S sequences using 500 Bootstrap replicates. The tree features four additional environmental 18S sequences (EF100276, EF100297, AY426928, AY789783) identified by blastn searches against Genbank. The red arrow points to the single clade grouping all *Olpidiopsis* and *Anisolpidium* sequences. The Bootstrap values are reflected by the diameter and colour of each node. Scale: number of nucleotide substitutions per site

584

585 **Supporting Information**

586 **Fig. S1** Additional captions of infected host algae

587 **Fig. S2** Additional *Olpidiopsis* sp. observed on a *Porphyra sp.* blade in Oban

588 **Fig. S3** 18S Phylogenetic tree (Maximum Parsominy)

589 **Fig. S4** Cox1 Phylogenetic trees

590 **Fig. S5** Cox2 Phylogenetic Trees

591 **Fig. S6** Intron Content in *Olpidiopsis porphyrae* varieties

592 **Fig. S7** Molecular characterization of some red algal hosts identified in this study

593 **Table S1** Summary table of all known *Olpidiopsis* sequences, OTUs described in this study, as
594 well as selected bibliographical records

595 **Table S2** List of all Genbank accessions used for 18S, Cox1, and Cox2 phylogeny reconstruction

596

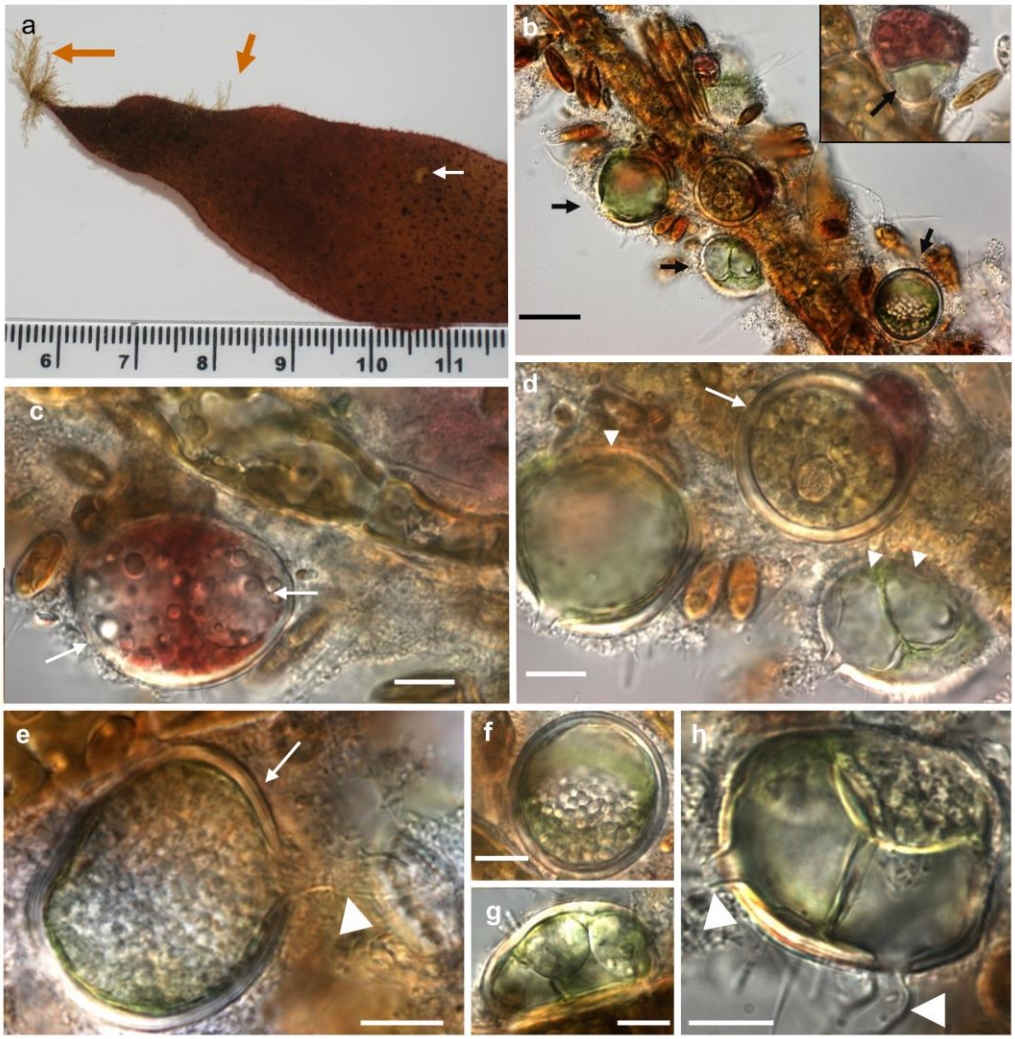

Fig.1 *Olpidiopsis palmariae* - Main description:

597

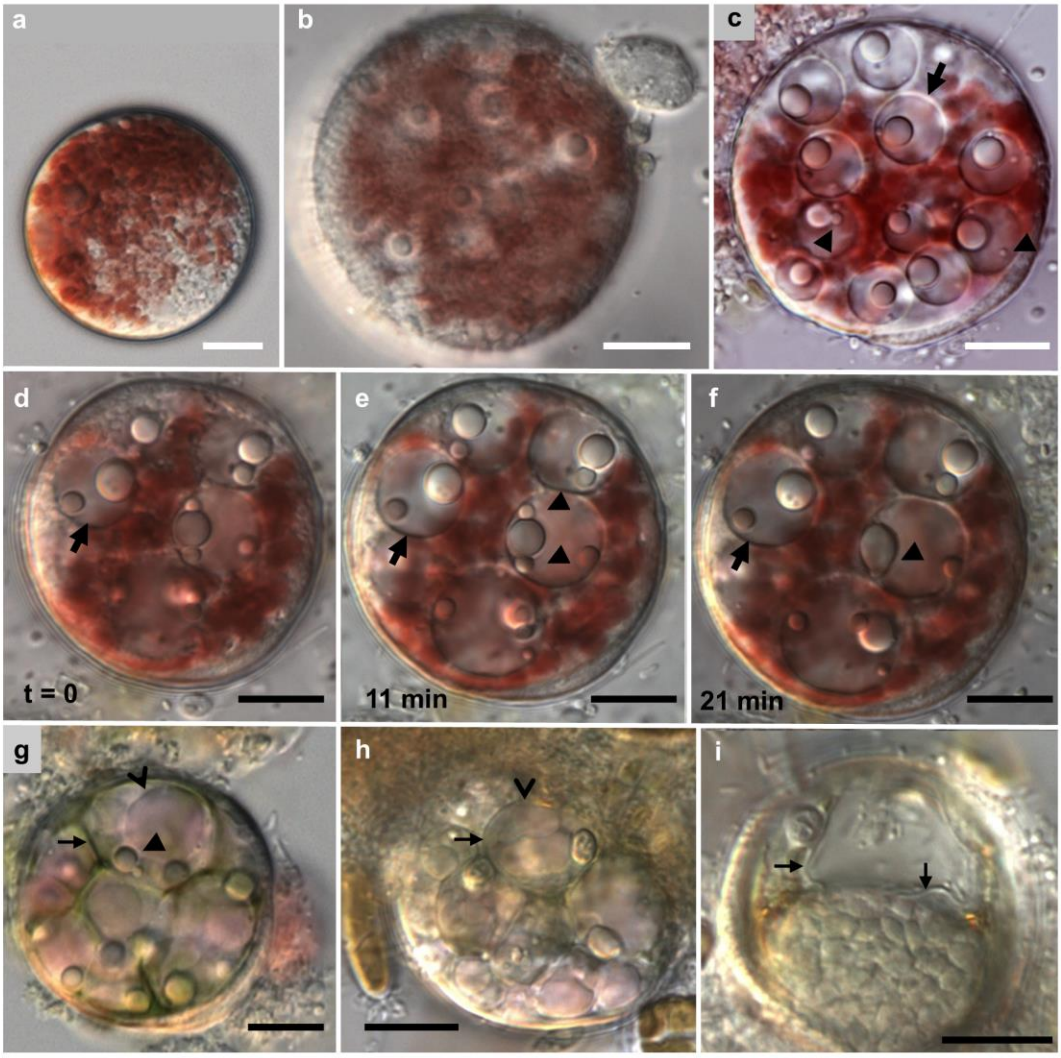

Fig.2 *Olpidiopsis palmariae* - Pathogen nutrition inside the tetraspore

598

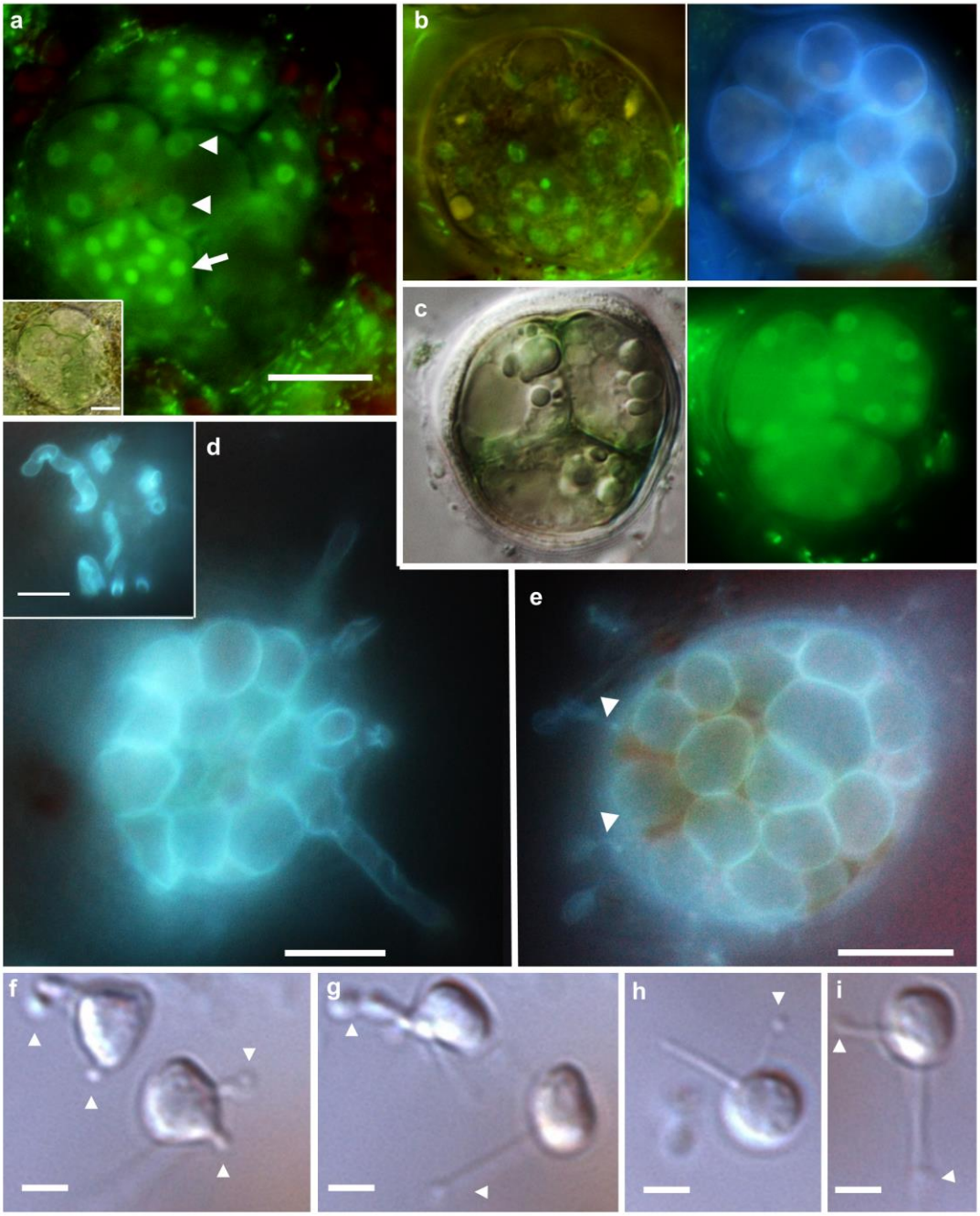

Fig.3. *Olpidiopsis palmariae* - sporogenesis and infection structures

599

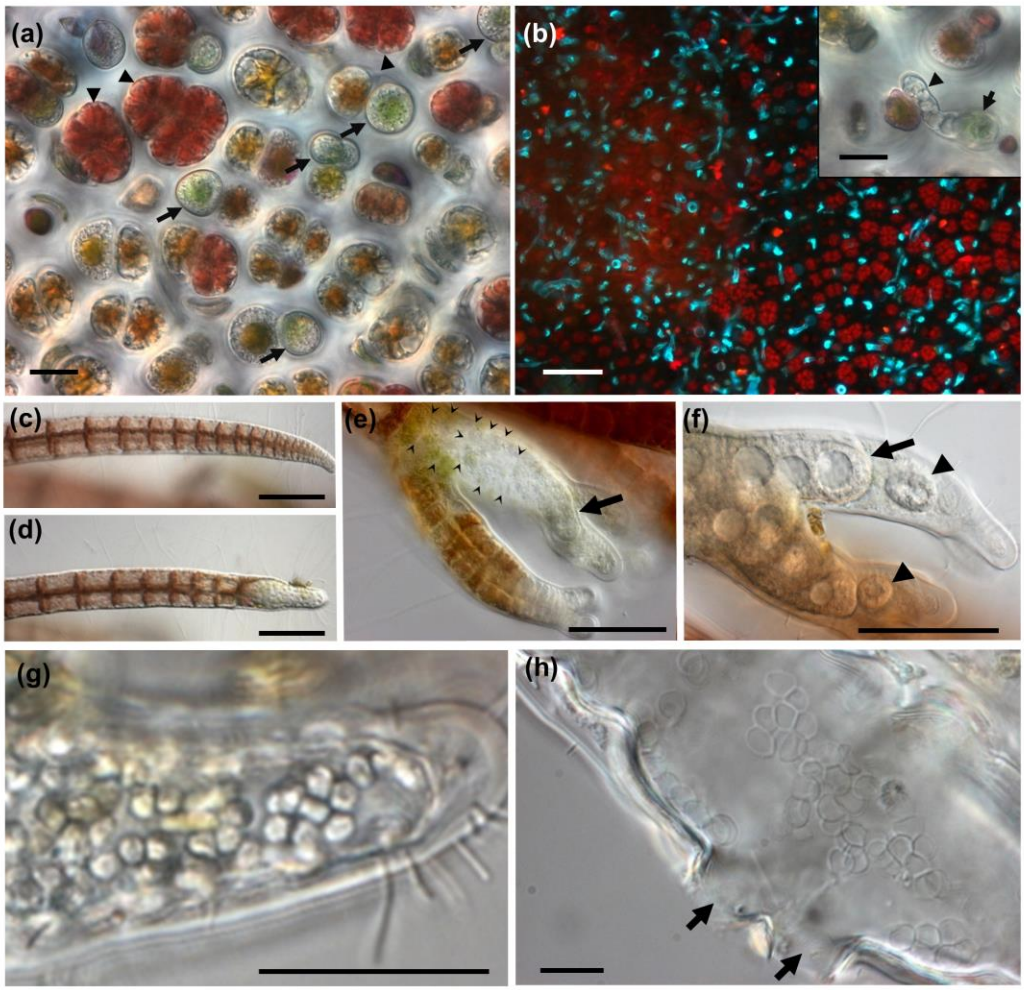

Fig. 4 *Olpidiopsis muelleri* sp. nov. on *Porphyra* sp. and *Polysiphonia* sp.

600

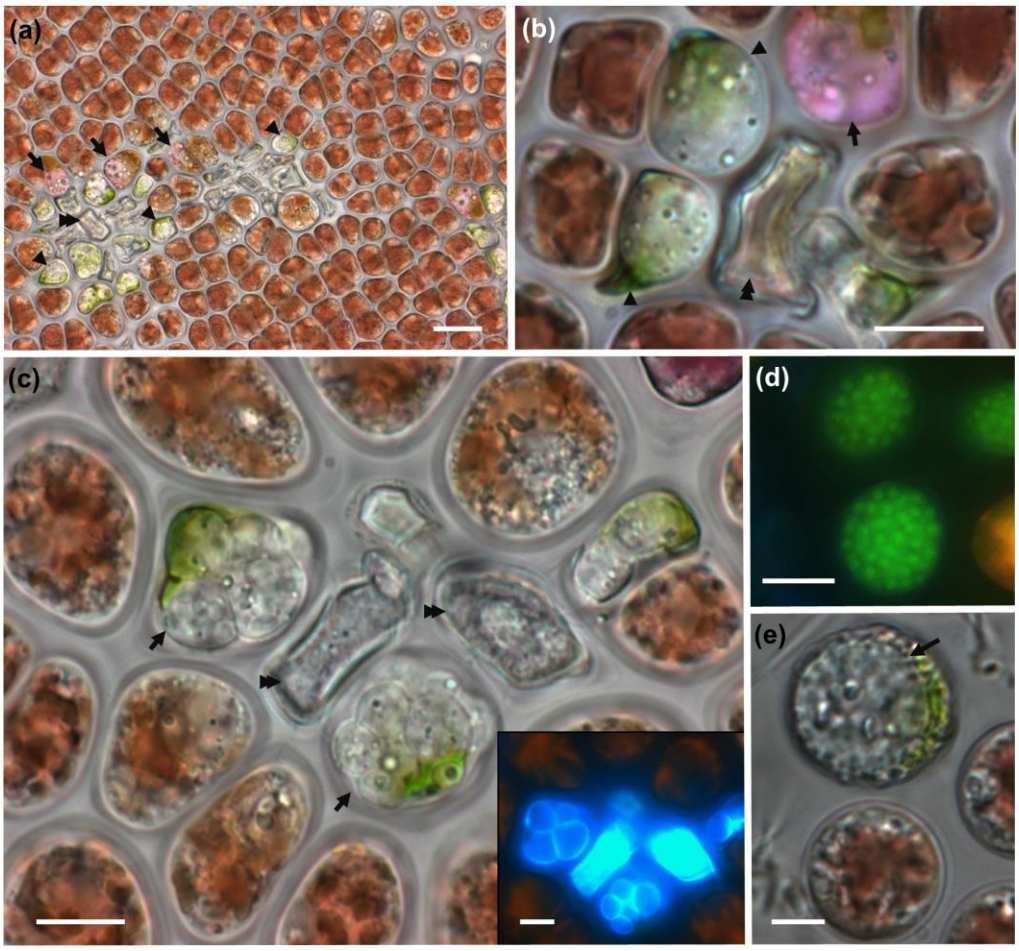

Fig. 5 *Olpidiopsis porphyrae* var. *scotiae* infecting *Porphyra* sp.

601

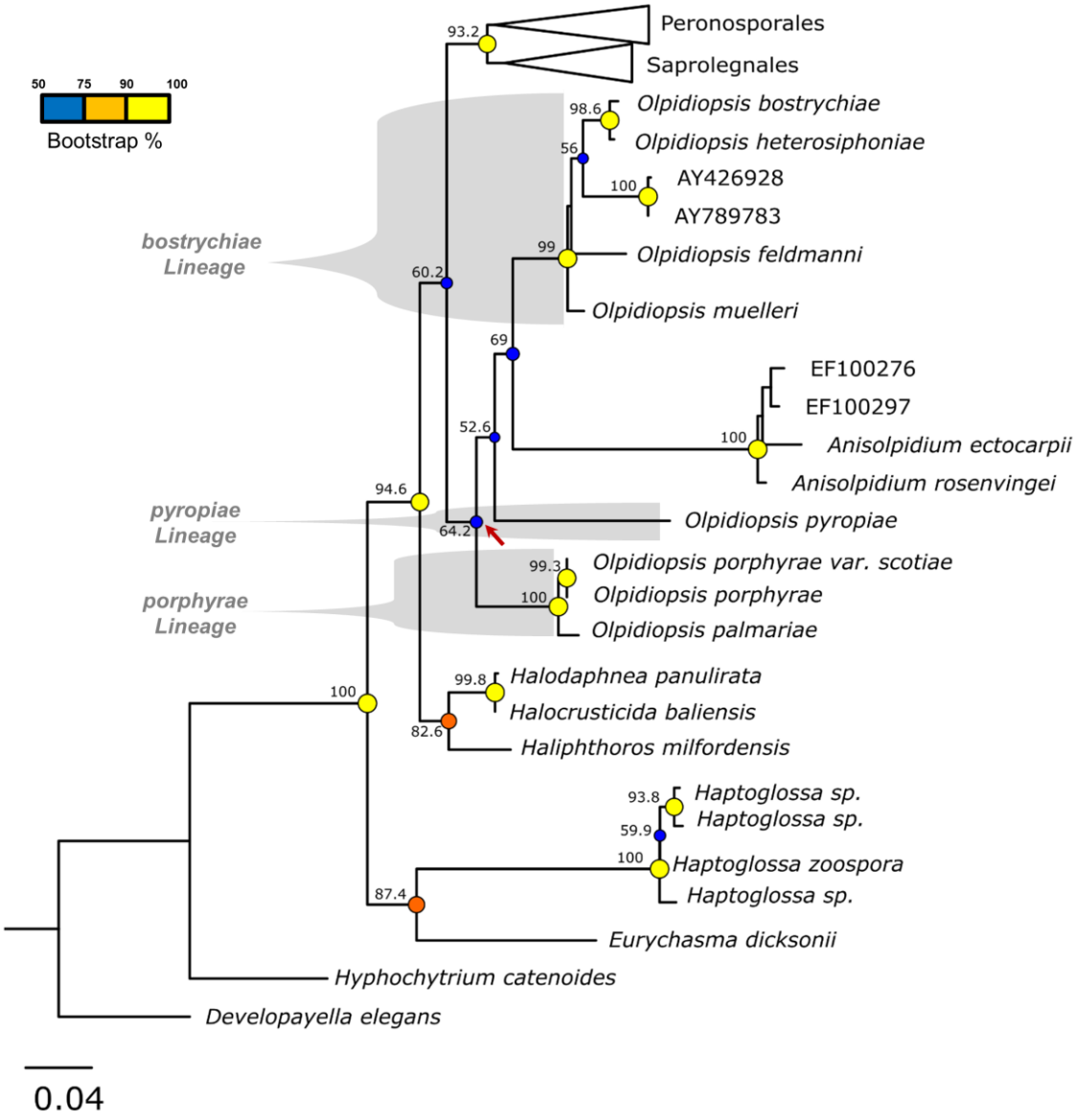
50 75 90 100
Bootstrap %
Peronosporales
Saprolegnales
Olpidiopsis bostrychiae
Olpidiopsis heterosiphoniae
AY426928
AY789783
Olpidiopsis feldmanni
Olpidiopsis muelleri
EF100276
EF100297
Anisolpidium ectocarpii
Anisolpidium rosenvingei
Olpidiopsis pyropiae
Olpidiopsis porphyrae var. scotiae
Olpidiopsis porphyrae
Olpidiopsis palmariae
Halodaphnea panulirata
Halocrusticida baliensis
Haliphthoros milfordensis
Haptoglossa sp.
Haptoglossa sp.
Haptoglossa zoospora
Haptoglossa sp.
Eurychasma dicksonii
Hyphochytrium catenoides
Developayella elegans
bostrychiae Lineage
pyropiae Lineage
porphyrae Lineage
93.2
98.6
56
100
99
60.2
69
52.6
100
94.6
64.2
99.3
100
99.8
100
82.6
93.8
59.9
100
87.4
0.04

Fig. 6

602